Advanced Functional Materials for the Detection of Perfluorinated Compounds in Water

Satya Ranjan Jena,[a] Sudesh Yadav,[b] AnchalYadav,[c] Bhavya M.B.,[a] Ali Altaee,[b]* Manav Saxena,[a] Akshaya K. Samal[a]*

[a]Centre for Nano and Material Sciences, Jain University, Ramanagara, Bangalore 562 112, Karnataka, India

[b] Centre for Green Technology, School of Civil and Environmental Engineering, University of

Technology Sydney, NSW 2007, Australia

[c] School of Chemistry, Monash University, Clayton, VIC-3800, Australia

Email: s.akshaya@jainuniversity.ac.in; Ali.Altaee@uts.edu.au

Abstract

Per- and polyfluoroalkyl substances (PFAS) are toxic and anthropogenic fluoro organic compounds found in the natural environment and living organisms, including humans. Numerous treatment methods have been investigated for these hazardous compounds, including physical, biological, and chemical processes. According to current trends, destructive treatment processes that result in the degradation and mineralisation of PFAS are the most desired by researchers and policymakers. Recently, nanomaterials have demonstrated their utility in a variety of applications, including energy, sensors, and separation technologies. However, their ability to degrade PFAS is still in its early stages.Thus, this chapter aims to provide valuable insights into various nanomaterials used for degradation of PFAS. Lastly, future research directions are suggested for a sustainable environment.

Keywords: Pre- and polyfluoroalkyl substances (PFAS), fluoro organic compounds, toxic, degradation, nanomaterials

1. Introduction

Globally, rapid urbanisation and increased industrialisation exacerbate a variety of environmental problems, including soil and water pollution[1, 2]. Emerging pollutants resulting from pesticides, industrial waste, flame retardants, detergents, and other organic compounds generated by humans pose a serious threat to future generations [3]. PFAS are examples of emerging contaminants that are extremely persistent in the human body and environment over an extended period due to their unique physicochemical properties such as confrontation to hydrolysis process, photolysis, and microbial degradation methods [4].

PFAS is a generic term used to describe very stable artificial perfluorinated chemicals (PFCs) that include perfluorooctanoic acid (PFOA), perfluorooctanesulfonic acid (PFOS), GenX, fluorotelomer alcohols(FTOHs), and over 4,000 other human-made chemicals. Originated in the United States in the 1940s, PFAs have been commercialized in the 1950s and are manufactured and used in various household and commercial products around the globe [5, 6]. The chemical structure of PFOA and PFOS is shown in **Figure 1**. The PFAS are generally made up of aliphatic compounds containing saturated C-F bonds with different carbon chain lengths and include varying amounts of oxygen and hydrogen.The C-F bond is highly stable and is resistant to chemical, physical, and biological degradation [7]. PFAs are also known as “forever chemicals” because once released into the environment, they do not break down and are absorbed in the human body, which accumulates in the human body with time. As compared to polyfluoroalkyl compounds (carbon chain with the presence of C-H bonds among C-F bonds), perfluoroalkyl compounds (fully fluorinated carbon chain) tend to be more persistent and toxic in the environment [6, 8]. Exposure to PFAs in water is primarily through ingestion, while the other household water usage is not significant. The contamination could occur from the release of PFAs to the industrial facility where PFAs are used for manufacturing the goods,

oil refineries where PFAs are used in firefighting equipment's, discharge from PFAs contaminated sewage treatment plants [4, 9, 10].

As a result, the European Commission has included PFOS to its list of critical elements, with an Environmental Quality Standards (EQS) of 0.65 ng/L for freshwater and 9.1 ng/L for biota (Directive 2013/39/EC) [11]. The Stockholm Convention's catalogue of emerging determined biological pollutants was supplemented in 2009 [12], and the US Environmental Protection Agency (EPA) included PFOS as incipient pollutants of alarm [13]. Because of their extended accumulation periods in the human body, both PFOS and PFOA, which were introduced before the 20th century, have been linked to obesity, cancer, hormone disruption, and high-fat levels [14, 15]. Evidence that significant sources of PFAS exist in Northern Italy, with significant impacts on surface and groundwaters, prompted the Italian government to form an employed assembly on EQS for PFAS compounds, to include some of them in the catalogue of international precise organic pollutants for superficial water observing and determining their presence [16, 17]. EQSs can protect freshwater bodies and marine habitats against the short- and long-term effects of organic contaminants, as well as human health when drinking water or many food items derived from aquatics. PFOS and PFOA are considered the most stable and do not degrade naturally in the environment.

According to the studies on the fate and behavior of these contaminants in wastewater treatment plants, biological treatment would be ineffective in their removal [18]. The addition of the adsorption process [19], sonochemical method [20], weakening with a zero-valent ion in less censorious and contaminated water [21], and membrane filtration process [22] are all well-known methods for removing perfluoroalkyl acids from drinking water processing. However, for PFAS degradation, UV-activated photoreduction [23], UV-photo decomposition [24], and the laccase-mediator reaction [25] are among the efficient methods available at present.

Recently, numerous nanomaterials are used for PFAS degradation from water. For instance, Wang et al. synthesized ferric-mediated ions that were then used to photocatalyze the degradation of PFOA using UV light with a wavelength of 254 nm [26]. They propose that PFOA forms a complex with the low-state ferric ion and that excitation with UV light at 254 nm causes PFOA to decompose in a stepwise fashion [26]. The current chapter began with a brief description of the occurrence of PFAS. The following section discusses the physical and chemical properties of PFAS, followed by a discussion of recent developments in the degradation of existing and emerging PFAS in water. Finally, future research directions and a summary of PFAS degradation technologies for a clean and sustainable environment are discussed.

2. Physical and chemical properties of PFAS

2.1. Physical properties

a) Physical state

The PFAS are generally solids, waxy solids, crystalline, or either used in powder form at room temperature (25 ℃) and one atmospheric pressure. However, the shorter chained compounds and, in particular, acid forms of perfluoroalkyl carboxylates and perfluroralkane sulfonates are liquids at room temperature. Like most organic compounds, the melting point of PFAS increases with the increase in the fluorinated chain length. For example, perfluorobutanoic acid (PFBA) has a melting point of 17.5 ° C, while perfluorododecanoic acid has 108-110 ℃ [27].

b) Density

Density plays a vital role in determining the behavior of the PFAS in the environment. If the density of the liquid PFAS is greater than that of water, it can migrate downward through the water column in groundwater or surface water as a dense non-aqueous phase liquid [27].

c) Solubility

Perfluoroalkyl compounds have a non-polar hydrophobic carbon chain as a fully saturated tail with fluorine atoms attached to a hydrophilic polar (nonfluorinated) functional group as the head. Due to this difference in head and tail, the PFAS aggregates into micelles, hemi micelles, or mixed micelles[9]. The PFAS form films at the air-water interface, with the hydrophobic carbon-fluorine tail oriented outwards and head dissolved in water. This enhances aerosol-based transportation and deposition while accumulation of PFAS at water surfaces. The micro dispersions of micelles are accounted while determining the solubility of PFAS.

The values for solubility of different PFAS (usually measured in milligrams per litres (mg/L) or moles per litres (mol/L)) may vary depending upon various factors such as the acid or salt used to determine the solubility, molecular weight, pH, salinity. For example, while PFOA and PFOS are highly soluble, the solubility of PFOA and PFOS tends to decrease with molecular weight, which is due to the concomitant increase in the length of the perfluorinated alkyl chains, which are hydrophobic [28].

d) Vapor Pressures (V_p)

Vapor pressure doesn't play a significant role in assessing the mobility and transportation of PFAS in the environment due to the very low vapour pressure of the PFAS. Compounds with higher vapor pressure are highly volatile and in the gaseous phase, converted to water vapors in the atmosphere and serve as transport media for long-range transport via air. For example, FTOH has varying vapor pressures, but compared with other PFAS, the vapor pressure of FTOHs is higher, making it a volatile compound. FTOH can be transformed to PFOA resulting in contamination of surface water and groundwater through precipitation. On the other hand, compounds with lower vapor pressures are less volatile and more likely to remain in solid or liquid form and can be transported via soil or surface/groundwater [29].

e) Henry's Law Constant (K_h)

The Henry's law constant (K_h), indicates the relative concentrations of a compound between an aqueous solution and gas phase at equilibrium (air-water distribution ratio). It is also useful in indicating the propensity of a chemical to remain dissolved in water as compared to volatilizing into the gas phase. PFAS with higher Henry's law constant will have lower solubility and higher volatility and can volatilize from water into the air and be distributed over a large area [30]. For most organic compounds of moderate to low solubility, K_h can be approximated evaluated using Equation 1:

$$K_h = (V_p)(M)/S \quad (1)$$

Where K_h is denoted as Henry's law constant, V_p is the vapor pressure, M is the molecular weight, and S is the solubility. PFAS dissociate into anions and cations, and Henry's law constant is pH-dependent. Since Henry's coefficients for the most PFAS are not known, the reported constants may not be applicable depending on the pH conditions within the solution.

2.2. Chemical properties

a) Carbon-Fluorine (C-F) Bonds

Due to the high electronegativity of fluorine and the presence of strong covalent C-F bonds, PFAs have shown very high chemical and thermal stabilities. They are resistant to degradation by oxidative and reductive processes involving the gain and loss of electrons. Furthermore, the low polarizability of fluorine gives the PFAs "amphiphilic" characteristics associating with both water and oils [31].

b) Functional Group

The functional groups of PFAS determine the properties and how PFAs should behave. The functional group in PFAS comprises carboxylates, sulfonates, sulfates, phosphates, amines,

and others [2]. The available experimental data and calculated pKa values indicate that both PFOA and PFOS are strong acids and are present as water-soluble anionic (deprotonated and negatively charged) forms environmentally relevant pH values. However, some PFAs are acids and may be present as cationic (protonated and positively charged) or a mixture of both called zwitterionic, depending on the pH of the environmental matrix and the compound's acid dissociation constant (pKa) [31]. Not just the C-F bond, the stability of PFAS is also determined by the specific functional group that is attached to the fluoroalkyl tail. PFOA and PFOS are the most stable fluorinated surfactants. PFAS decomposes at temperatures greater than 400 °C, but complete mineralization occurs at temperatures greater than 1000 °C [32].

3. Degradation of PFAS

Due to the fact that PFC degradation produces additional toxic and harmful byproducts, integrated techniques using absorption by functionalized nanomaterials (such as powdered activated carbon, carbon nanotubes, functionalized polymers, and resins) is widely investigated [33, 34]. While the literature supports using high-performance absorbents for long-chain PFAS, it remains devoid of integration with real-time degradation methods[35]. Niu and colleagues synthesised sonicated graphene quantum dots (GQDs) for the decomposition of PFOS compounds. Also, the authors synthesised SiC/GQDs due to their superior and excellent activity compared to bare GQDs. **Figure 2a** illustrates the highly uniform surface topology of SiC/GQDs in the presence of homogeneous GQDs with a size range of 1.8-3.6 nm embedded in SiC nanoparticles. **Figure 2a also** illustrates the mechanism of PFOS degradation via directional electron transfer using SiC/GQDs. The decomposition experiment was conducted using a nanocomposite containing 0.019 mmol/L PFOS and 40 mg SiC/GQDs. When the photochemical electrons are directly attached to the PFOS molecule, delocalization of the electron pair attached to the sulphur atom occurs due to the lone pair attached to the sulphur atom. Following that, the SO_2 radical accepts the H^+ ion to eliminate OH^- ions. Then, through

the addition of HF and hydrolysis, it is converted to the carboxylic (COOH) compound carbon-fluoride (C_nF_{2n-1}) [36]. Finally, the C_nF_{2n-1}-COOH dissociated completely to form C_nF_{2n-1} and CO_2 (**Figure 3**). UV radiation triggers the dissociation of carbon fluoride bonds[36]. The UV-Visible spectrum analysis of the GQDs nanocomposite is shown in **Figure 2b**. UV-Visible spectral analysis reveals peaks at 310 and 340 nm. The 340 nm absorption peak corresponds to the nonbonding and π* orbitals (n-π*), while the 310 nm absorption peak corresponds to π-π* orbital. These corresponding absorbance peaks appear on the same fluorescence emission-excitation map as the PL excitation. In PLE spectral analysis, two prominent electronic transitions at 260 nm (4.77 eV, Peak A) and 310 nm (4.00 eV, Peak B) were detected (**Figure 2c**). To determine the crystallographic structure of nanomaterials, XPS spectrum analysis was used, and C1s exhibits peaks at 282.8 eV, 284.8 eV, 286.0 eV, and 288.8 eV corresponding to Si–C, C=C, C–O, and C=O bonds, respectively. Numerous factors contribute to the stability of the GQDs molecules on the surface of the SiC molecule. Between those variables, the surface oxygen-containing functional layer plays a critical role. SiC/GQDs are completely stabilised in the presence of that surface oxygen. The PFOA and its substitutes, such as $C_3F_7COO^-$ (PFBA), $C_4F_9COO^-$ (PFPeA), $C_5F_{11}COO^-$ (PFHxA), and $C_6F_{13}COO^-$ (PFHpA), are photochemically degraded using a stabilised SiC/GQDs nanocomposite. These results were obtained at room temperature (25 °C) using triple-stage quadrupole mass spectrometry (TQ-MS/MS). Accordingly, the detection times for the PFOS substituents are 1.99, 2.36, 2.95, 3.76, and 4.64 minutes, respectively. The PFOS and its substituents are detected and decomposed in time variations using zero-dimensional and semiconductor SiC/GQDs [36].

Later, Huang and co-researchers also demonstrated that PFOS degradation could be achieved through the reactive electrochemical membrane (REM) using a responsive porous Magneli phase titanium suboxide ceramic membrane nanomaterial [37]. By employing REM, it was possible to obtain complete removal of PFOS, 98.30 %, which was achieved using an anodic

potential of 3.15 V vs a standard hydrogen electrode (SHE). The crystallographic structure of the magneli phase titanium suboxide ceramic membrane is shown in **Figure 4a**. The characteristic peaksof Ti_9O_{17}, Ti_6O_{11}, and TiO_2 indicate that the primary component of this TSO mixture is Ti_9O_{17}. **Figure 2b** illustrates the surface topology of a titanium suboxide ceramic membrane, which reveals an extensive pore network on the anode surfaces; additionally, the calculated pore size is close to 0.5 - 3 µm. Purposive experiments in conjunction with density functional theory (DFT) computations were used to investigate the reaction's performance, routes, and mechanisms. The concentration of linear PFOS (L-PFOS) vs applied current densities in the presence of a reactive electrochemical membrane is depicted in **Figure 2c**. The concentration of linear PFOS (L-PFOS) vs applied current densities in the presence of a reactive electrochemical membrane is depicted in **Figure 2c**. According to multiple reaction monitoring, the ratio of L-PFOS to branched PFOS (B-PFOS) is 16.5. Once an electric current is applied to the system, it increases the current density while simultaneously decreasing the PFOS concentration. By 120 minutes, a significant amount of PFOS concentration was removed, 98.30% at 4 $mAcm^{-2}$. The author conducts a comparison experiment with varying current densities in the presence of a solution of 2 µM PFOS in 100mM of Na_2SO_4. The reaction mechanism is shown in **Figure 2d**. When the current density is increased simultaneously, the PFOS concentration decreases, mimicking REM conditions. The linear scan voltammetry of a 100mM of Na_2SO_4 solution with varying concentrations of PFOS. At a scan rate of 20 mV/s, no increase in peak in electric current was observed upon PFOS addition, even though the applied current decreased with increasing concertation of the PFOS amount. Using DFT to calculate the electrode potential, the energy profile values of 2.96 and 3.24 vs SHE are obtained experimentally. This may indicate that the contribution of $\bullet OH_{dis}$to PFOS degradation on the Ebonex anode during EO is limited compared to the surface-bound $\bullet OH_{ads}$[37].

In another study, Li and coworkers used the solvothermal process to synthesise In_2O_3 nanostructures with a variety of shapes. They have synthesised various structures such as microspheres, nanocubes, and nanoplates using different reducing agents and temperatures[38]. The atomic structure of PFOA plays a significant role in the catalytic degradation process [39], particularly in the case of increased activity. Additionally, the varying sizes and shapes of In_2O_3 play a significant role in the PFOA degradation process [38]. When it comes to degradation activity, In_2O_3 microspheres outperform nanocubes and nanoplates. **Figure 5a** illustrates how the surface topology of In_2O_3 microspheres with a diameter of approximately 180 nm results in the formation of small nanoparticles of 15-20 nmdiameter. Sincecalcination is a homogeneous process, the smaller particles aggregate to form the larger particle. The surface morphology of In_2O_3nanocubes and nanoplates is depicted in **Figures 5b** and **c**, respectively. In **Figure 5b**, the In_2O_3nanocubes are shown in their natural state, but their structure is not perfectly cube-like, whereas, in **Figure 5c**, they show a uniform nanoplates-like structure. **Figure 5d** shows UV-Visible spectral analysis of In_2O_3 nanostructures of various shapes. The band gaps of In_2O_3 microspheres, nanocubes, and nanoplates corresponding to 2.68, 2.76, and 2.72 eV, respectively. XPS spectral analysis reveals that different nanostructures exhibit the same binding energy peaks. The current peaks at 444.2 and 451.7 correspond to the $3d_{5/2}$ and $3d_{3/2}$ levels of In. Overall, due to the high concentration of surface oxygen in In_2O_3 nanomaterials, they exhibit a greater range of photocatalytic activity than TiO_2 and $P_{25}TiO_2$. The UV results demonstrate that PFOA decomposition occurs at a wavelength of 254 nm or greater (**Figure 5d**). In this experiment, In_2O_3 microspheres outperformed nanoplates, nanocubes, and TiO_2 in terms of photocatalytic activity. However, in the case of TiO_2, only 28.5 % decomposition occurs in three hours. Contrary, microspheres take 20 minutes to decompose, nanoplates and nanocubes take 40 and 120 minutes, respectively, to decompose the PFOA mixture. The decomposition of PFOA was

the pseudo-first-order reaction. As with PFOA, the In_2O_3 microspheres exhibit superior photocatalytic activity compared to the In_2O_3 nanoplates and nanocubes. Further, the standardisation and time dependence study of the photocatalytic decomposition of perfluoro carboxylic acids (PFCAs), including perfluoro heptanoic acid (PFHpA), perfluoro hexanoic acid (PFHpA), perfluorononanoic acid (PFPeA), perfluoro butanoic acid (PFBA), and trifluoroacetic acid (TFA) in the presence of noble In_2O_3 microspheres [38]. Results showed that In_2O_3 microspheres have a high potential for real-time degradation processes. However, process optimization is still at an early stage.

4. Future research directions and summary

While several technologies have been investigated for the degradation of PFASs in the environment and, more specifically, wastewater. This review has concentrated on treatment methods that utilize nanomaterials in the degradation process. AOPs based on photolysis and photocatalysis are still being developed for the degradation of PFAS. Photolysis is a low-energy process (99.2 KWh/m^3) with a moderate removal efficiency of 82 %. In comparison, the photocatalysis process achieves 89 % removal efficiency but consumes a lot of energy (2106 KWh/m^3). In comparison to previously reported AOPs, the advanced reduction process (ARPs) is still in the research stage and achieves a removal efficiency of 91.4 % with relatively low energy consumption (166.1 KWh/m^3) [40]. However, the low yield and lack of efficient methods for generating e_{aq}^- in ARPs continue to be a challenge.

Among semiconductor-based nanomaterials such as TiO_2 and various shapes of In_2O_3, In_2O_3 microspheres demonstrated the highest degradation activity and can be further investigated in future studies. Additionally, while iron-based photochemical processes are effective for advanced oxidation, further degradation of toxic byproducts and short-chain PFAS remains a challenge. To conclude, PFAS degradation pathways are highly dependent on their head

groups. Fluoroalkyl chain lengths may also affect the reductive degradation patterns of specific PFAS types. The degradation and defluorination efficiencies of PFAS are strongly influenced by solution chemistry parameters and operating factors such as pH, the dose of chemical solute (i.e., sulphite or iodide) used for dissolved oxygen, humic acid, and nitrate, and temperature. In general, future research should focus on developing energy-efficient and economically viable methods for completely degrading PFAS without producing secondary waste. Hybrid methods are still in their infancy, and a thorough techno-economic analysis is required to develop sustainable technology.

Figures

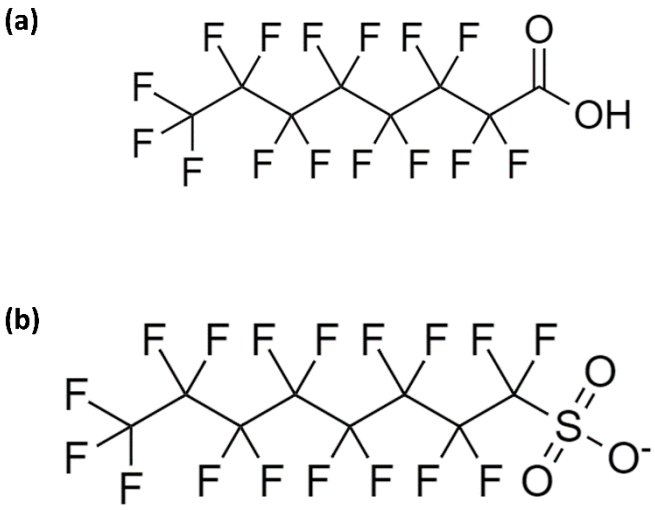

Figure 1. Chemical structure of (a) PFOA and (b) PFOS.

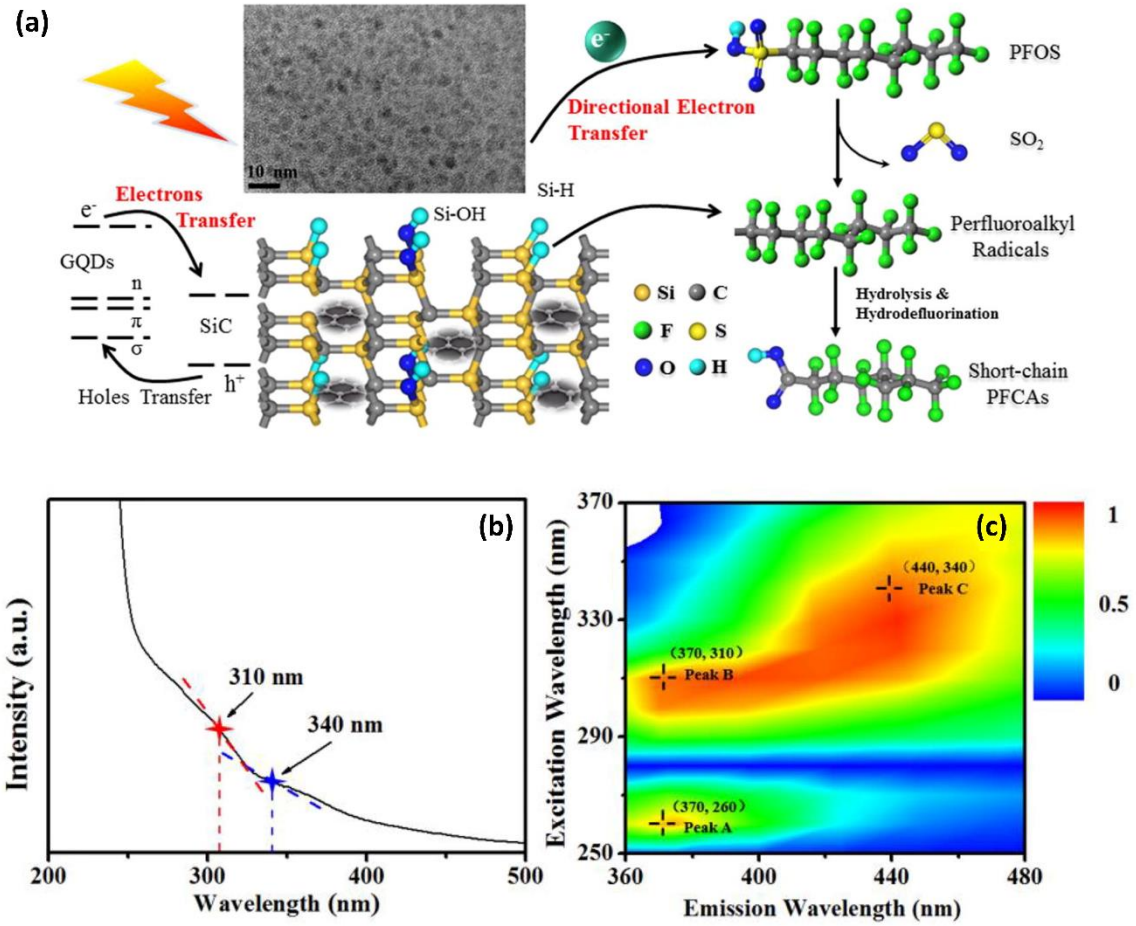

Figure 2. (a) SEM morphology and reaction mechanism (Directional electron transfer) of SiC/GQDs reaction with PFOS and its substituents, (b) UV-Visible spectral analysis of SiC/GQDs nanocomposite, and (c) PL spectra of SiC/GQDs nanocomposite analysis on fluorescence emission-excitation map [36].

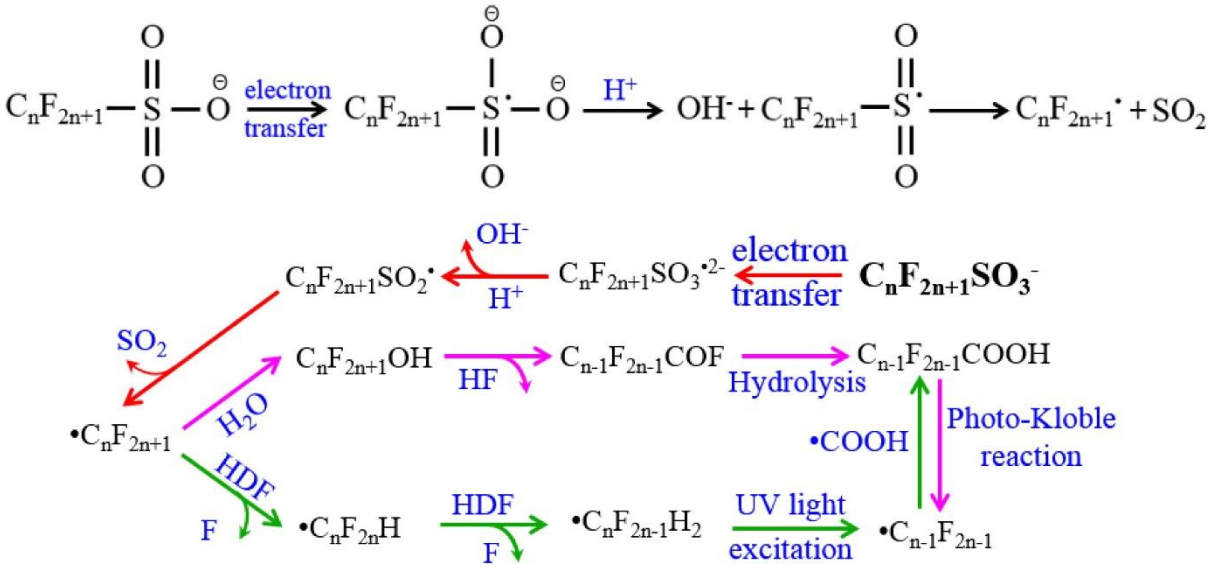

Figure 3. Proposed decomposition mechanism for PFOS using SiC/graphene [36].

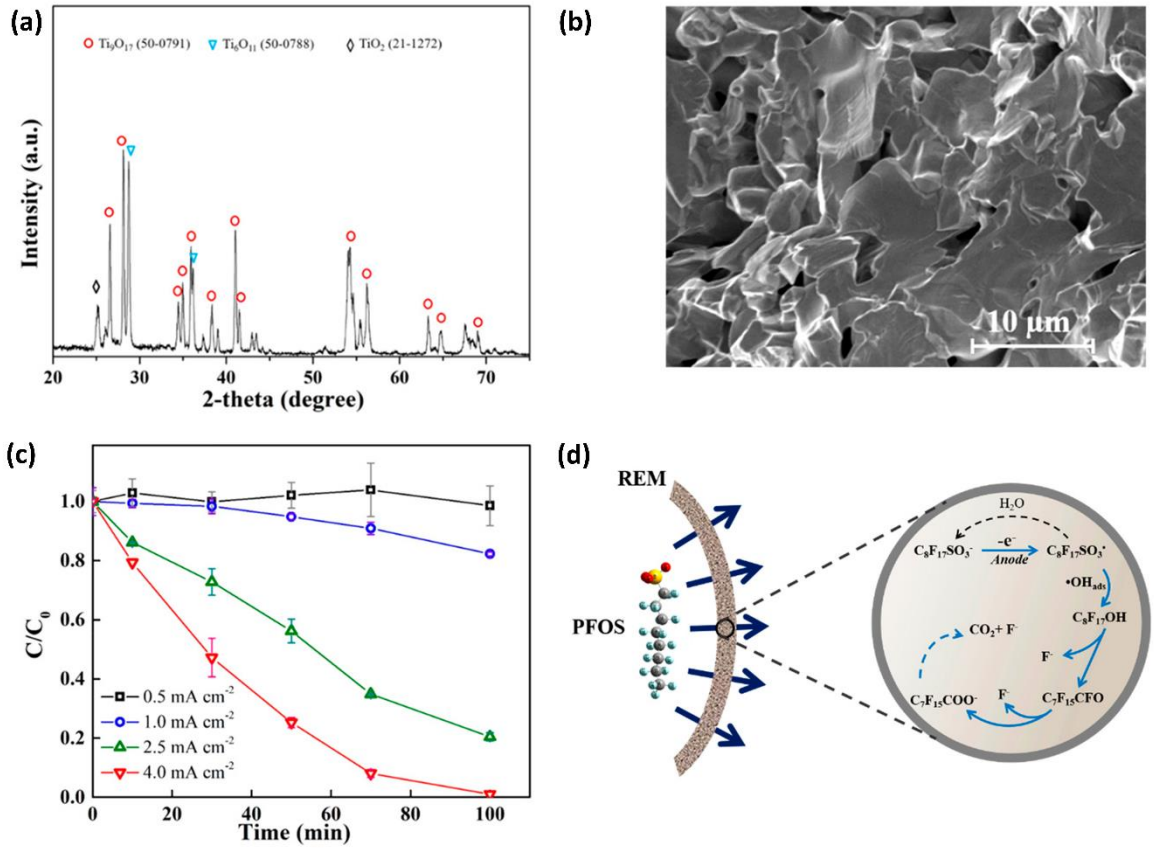

Figure 4. (a) XRD pattern of Ebonex anode material (Magneli phase titanium suboxide ceramic membrane nanomaterial), (b) SEM morphology of anode material, (c) L-PFOS

concentration profiles in group EO system at unalike current density (0.5 – 4.0 mA cm^{-2}), and (d) reaction mechanism of PFOS degradation using REM membrane. [37].

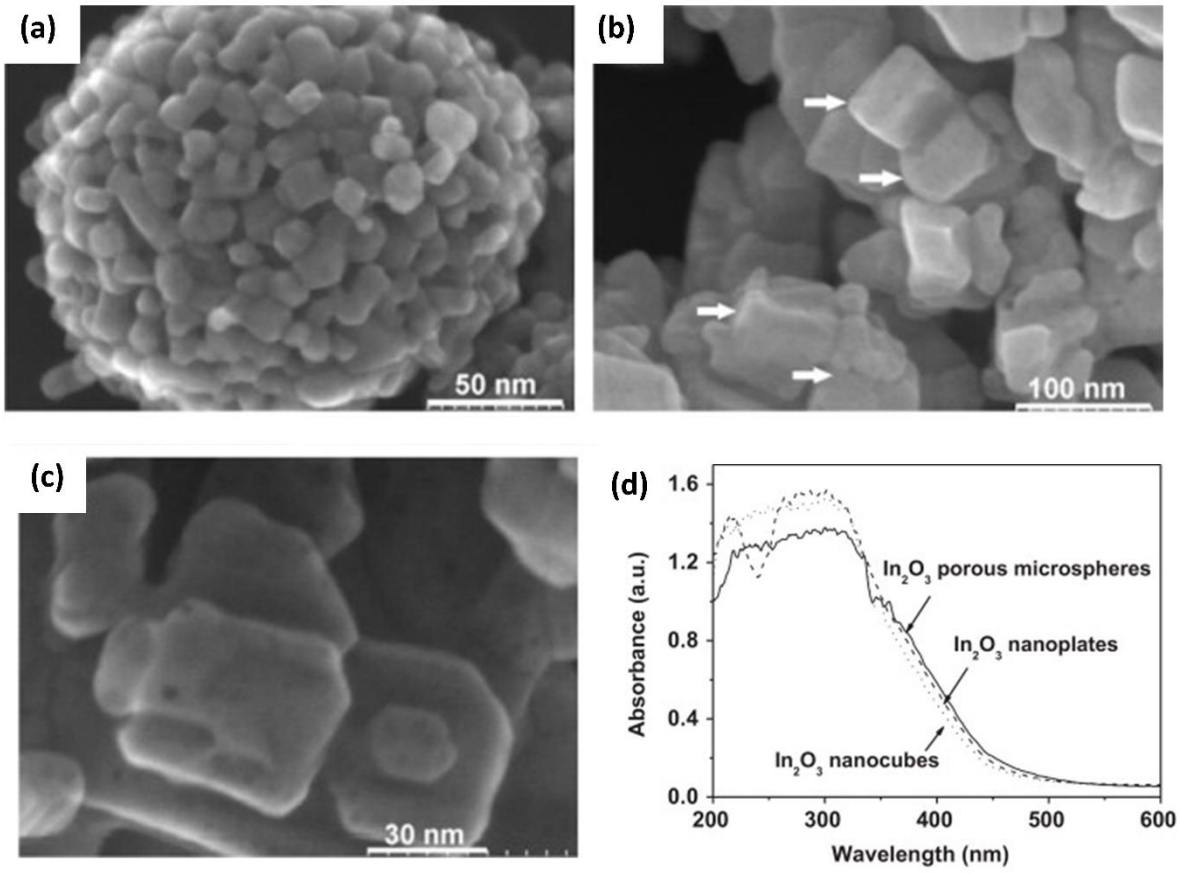

Figure 5. SEM morphology different shapes of In_2O_3 nanostructures, (a) In_2O_3 microspheres, (b) In_2O_3 nanocubes, and (c) In_2O_3 nanoplates. (d) UV-Visible spectral analysis of In_2O_3 nanostructures.

References

1. Bhol, P., et al., *Graphene-based membranes for water and wastewater treatment: A Review.* ACS Applied Nano Materials, 2021. **4**(4): p. 3274-3293.
2. Yadav, S., et al., *Recent developments in forward osmosis membranes using carbon-based nanomaterials.* Desalination, 2020. **482**: p. 114375.
3. Tang, Y., et al., *Emerging pollutants in water environment: Occurrence, monitoring, fate, and risk assessment.* Water Environment Research, 2019. **91**(10): p. 984-991.
4. Hogue, C., *How to say goodbye to PFAS.* Chemical & Engineering News, 2019. **97**(46): p. 22-25.
5. Nakayama, S.F., et al., *Worldwide trends in tracing poly-and perfluoroalkyl substances (PFAS) in the environment.* TrAC Trends in Analytical Chemistry, 2019. **121**: p. 115410.
6. Buck, R.C., et al., *Perfluoroalkyl and polyfluoroalkyl substances in the environment: terminology, classification, and origins.* Integrated environmental assessment and management, 2011. **7**(4): p. 513-541.
7. Smart, B.E., *Characteristics of CF systems*, in *Organofluorine Chemistry*. 1994, Springer. p. 57-88.
8. Kah, M., D. Oliver, and R. Kookana, *Sequestration and potential release of PFAS from spent engineered sorbents.* Science of The Total Environment, 2020: p. 142770.
9. Ross, I., et al., *A review of emerging technologies for remediation of PFASs.* Remediation Journal, 2018. **28**(2): p. 101-126.
10. Dean, W.S., et al., *A Framework for Regulation of New and Existing PFAS by EPA.* J. Sci. Policy Governance, 2020. **16**.
11. Valsecchi, S., et al., *Deriving environmental quality standards for perfluorooctanoic acid (PFOA) and related short chain perfluorinated alkyl acids.* Journal of hazardous materials, 2017. **323**: p. 84-98.
12. Wang, T., et al., *Perspectives on the inclusion of perfluorooctane sulfonate into the Stockholm convention on persistent organic pollutants*. 2009, ACS Publications.
13. Post, G.B., P.D. Cohn, and K.R. Cooper, *Perfluorooctanoic acid (PFOA), an emerging drinking water contaminant: a critical review of recent literature.* Environmental research, 2012. **116**: p. 93-117.
14. Betts, K.S., *Perfluoroalkyl acids: what is the evidence telling us?* 2007, National Institute of Environmental Health Sciences.

15. Jian, J.-M., et al., *Global distribution of perfluorochemicals (PFCs) in potential human exposure source–a review.* Environment international, 2017. **108**: p. 51-62.
16. Castiglioni, S., et al., *Sources and fate of perfluorinated compounds in the aqueous environment and in drinking water of a highly urbanized and industrialized area in Italy.* Journal of hazardous materials, 2015. **282**: p. 51-60.
17. Valsecchi, S., et al., *Occurrence and sources of perfluoroalkyl acids in Italian river basins.* Chemosphere, 2015. **129**: p. 126-134.
18. Yu, J., et al., *Perfluorooctane sulfonate (PFOS) and perfluorooctanoic acid (PFOA) in sewage treatment plants.* Water research, 2009. **43**(9): p. 2399-2408.
19. Hansen, M.C., et al., *Sorption of perfluorinated compounds from contaminated water to activated carbon.* Journal of Soils and Sediments, 2010. **10**(2): p. 179-185.
20. Moriwaki, H., et al., *Sonochemical decomposition of perfluorooctane sulfonate and perfluorooctanoic acid.* Environmental science & technology, 2005. **39**(9): p. 3388-3392.
21. Hori, H., et al.,*Efficient decomposition of environmentally persistent perfluorooctanesulfonate and related fluorochemicals using zero-valent iron in subcritical water.* Environmental science & technology, 2006. **40**(3): p. 1049-1054.
22. Tang, C.Y., et al., *Use of reverse osmosis membranes to remove perfluorooctane sulfonate (PFOS) from semiconductor wastewater.* Environmental science & technology, 2006. **40**(23): p. 7343-7349.
23. Sun, Z., et al., *Impact of humic acid on the photoreductive degradation of perfluorooctane sulfonate (PFOS) by UV/Iodide process.* Water research, 2017. **127**: p. 50-58.
24. Jin, L., et al., *Ferric ion mediated photodecomposition of aqueous perfluorooctane sulfonate (PFOS) under UV irradiation and its mechanism.* Journal of hazardous materials, 2014. **271**: p. 9-15.
25. Luo, Q., et al., *Perfluorooctanesulfonate degrades in a laccase-mediator system.* Environmental science & technology, 2018. **52**(18): p. 10617-10626.
26. Wang, Y., et al., *Ferric ion mediated photochemical decomposition of perfluorooctanoic acid (PFOA) by 254 nm UV light.* Journal of Hazardous Materials, 2008. **160**(1): p. 181-186.
27. Rahman, M.F., S. Peldszus, and W.B. Anderson, *Behaviour and fate of perfluoroalkyl and polyfluoroalkyl substances (PFASs) in drinking water treatment: A review.* Water research, 2014. **50**: p. 318-340.

28. Nguyen, T.M.H., et al., *Influences of Chemical Properties, Soil Properties, and Solution pH on Soil–Water Partitioning Coefficients of Per-and Polyfluoroalkyl Substances (PFASs).* Environmental Science & Technology, 2020. **54**(24): p. 15883-15892.
29. Berger, U., et al., *Recent developments in trace analysis of poly-and perfluoroalkyl substances.* Analytical and bioanalytical chemistry, 2011. **400**(6): p. 1625-1635.
30. Johansson, J.H., et al., *Water-to-air transfer of branched and linear PFOA: Influence of pH, concentration and water type.* Emerging Contaminants, 2017. **3**(1): p. 46-53.
31. Sznajder-Katarzyńska, K., M. Surma, and I. Cieślik, *A review of perfluoroalkyl acids (PFAAs) in terms of sources, applications, human exposure, dietary intake, toxicity, legal regulation, and methods of determination.* Journal of Chemistry, 2019. **2019**.
32. Lassen, C., et al., *Survey of PFOS, PFOA and other perfluoroalkyl and polyfluoroalkyl substances.* Part of the LOUS-review. Environmental Project, 2013(1475).
33. Lin, H., et al., *Electrochemical degradation of perfluorooctanoic acid (PFOA) by Ti/SnO_2-Sb, Ti/SnO_2-Sb/PbO_2 and Ti/SnO_2-Sb/MnO_2 anodes.* Water research, 2012. **46**(7): p. 2281-2289.
34. Xiao, L., et al., *β-Cyclodextrin polymer network sequesters perfluorooctanoic acid at environmentally relevant concentrations.* Journal of the American Chemical Society, 2017. **139**(23): p. 7689-7692.
35. Zhang, W., D. Zhang, and Y. Liang, *Nanotechnology in remediation of water contaminated by poly-and perfluoroalkyl substances: A review.* Environmental pollution, 2019. **247**: p. 266-276.
36. Huang, D., et al., *Directional electron transfer mechanisms with graphene quantum dots as the electron donor for photodecomposition of perfluorooctane sulfonate.* Chemical Engineering Journal, 2017. **323**: p. 406-414.
37. Shi, H., et al., *Degradation of perfluorooctanesulfonate by reactive electrochemical membrane composed of magneli phase titanium suboxide.* Environmental science & technology, 2019. **53**(24): p. 14528-14537.
38. Li, Z., et al., *Different nanostructured In_2O_3 for photocatalytic decomposition of perfluorooctanoic acid (PFOA).* Journal of hazardous materials, 2013. **260**: p. 40-46.
39. Zhang, J., et al., *Stabilization of platinum oxygen-reduction electrocatalysts using gold clusters.* Science, 2007. **315**(5809): p. 220-222.
40. Olatunde, O.C., A.T. Kuvarega, and D.C. Onwudiwe, *Photo enhanced degradation of polyfluoroalkyl and perfluoroalkyl substances.* Heliyon, 2020. **6**(12): p. e05614.